W-boson electric and weak-electric dipole moments and helicity amplitudes in $f_i\bar{f}_j \to W^{\pm}\gamma$ or Z^0

J. Garcia and A. Queijeiro
Departamento de Física, Escuela Superior de Física y Matemáticas, Instituto Politécnico Nacional, Edificio 9, Unidad Profesional Adolfo López Mateos, 07738 México D.F., Mexico
e-mail: aquei@esfm.ipn.mx

Recibido el 23 de abril de 1998; aceptado el 11 de junio de 1998

We study the possibility of measuring the CP-odd electric and weak-electric dipole moments (edm and wedm, respectively) of the W-boson through an analysis of the helicity amplitudes in the process $f_i\bar{f}_j \to W^{\pm}V (V = \gamma \text{ or } Z^0)$, where f_i and f_j are elementary fermions. We show that, for example, for the initial state $e\bar{\nu}_e$, such moments can be detected in the angular distribution of the final state pair when their helicities are $(0, \pm)$ for $V = \gamma$, or $(\pm, 0)$ and $(0, \pm)$ for $V = Z^0$.

Keywords: W-boson; weak-electric dipole moment; helicity amplitudes

Estudiamos la posibilidad de medir tanto el momento dipolar eléctrico del boson W, así como su momento dipolar débil eléctrico a través del análisis de las amplitudes de helicidad del proceso $f_i\bar{f}_j \to W^{\pm}V (V = \gamma \text{ o } Z^0)$, donde f_i y f_j son fermiones elementales. Mostramos por ejemplo, que si consideramos inicialmente $e\bar{\nu}_e$, tales momentos pueden ser detectados en la distribución angular del estado final cuando sus helicidades son $(0, \pm)$ para $V = \gamma$, o $(\pm, 0)$ y $(0, \pm)$ para $V = Z^0$.

Descriptores: Boson W; momento dipolar débil eléctrico; amplitudes de helicidad

PACS: 14.80.Er; 12.15.Ji; 12.50.Fk

1. Introduction

An aspect of the standard model (SM) of electroweak unification, based on the gauge group $SU(2)_L \times U(1)_Y$, to be tested experimentally is the three-vector boson couplings $WW\gamma$ and WWZ. The explicit tensor nature of these vertices is a consecuence of the gauge structure of the model. The vertices, in turn, are responsible for the characteristic electroweak properties of the spin one elementary charged W boson, the (weak) electric and magnetic multipole moments. In particular its electric dipole moment (edm) is predicted to be quite small, arising at the three loop level [1]; an expected result since this moment does not respect the CP symmetry. Using the experimental value for the neutron edm, the corresponding edm value for the W boson, $d_\gamma = e\tilde{\kappa}_\gamma/2M_W$, is bounded by [2] $\tilde{\kappa}_\gamma \leq 10^{-3}$. It is expected that the analogous CP violating weak edm, $d_Z = e\tilde{\kappa}_Z/2\cos\theta_W M_W$ be also bounded by [3] $\tilde{\kappa}_Z \leq 10^{-3}$. On the contrary, the CP-even (weak) magnetic dipole moment $\mu_V = e_V(1 + \kappa_V + \lambda_V)/2M_W$, and the (weak) electric quadrupole moment $Q_V = e_V(\kappa_V - \lambda_V)/M_W^2$, with $\kappa_V = 1+$ radiative corrections and $\lambda_V = 0+$ radiative corrections are expected to dominate in processes where the complete vertex $WWV (V = \gamma \text{ or } Z^0)$ is taken into account. This is so when the resulting cross-section is summed over all helicity states. The situation is different when we compute definite helicity amplitudes, as we show in this work.

The method of helicity amplitudes has been used to study anomalous couplings of the W boson; for instance, in the reaction $f_i\bar{f}_j \to W^{\pm}\gamma$ where f_i and f_j belongs to an $SU(2)_L$ isodoublet of elementary fermions, it was shown [4] that the amplitude exhibits, at the Born level, a zero. Anomalous couplings spoil that zero, indicating a possible non elementary nature of the gauge bosons. Other related processes, like [5] $W \to ff'\gamma$, also exhibit this zero. Recently Baur *et al.* [6] studied the process $f_i\bar{f}_j \to W^{\pm}Z$, for CP even anomalous couplings, showing that the amplitude exhibits an approximate zero. One can see that the helicity amplitudes $\Delta M(h_W, h_V)$ coming from the SM couplings and the anomalous CP-even couplings, $\Delta\kappa_V = 1 - \kappa_V$ and λ_V, factorizes with factors $(1 \mp \cos\theta)$ and $(1 \pm \cos\theta)$, for helicities $(\pm, 0)$ and $(0, \pm)$, respectively, where h_W and h_V are the helicities of the W and V bosons, and θ is the center of mass scattering angle of the W-boson. This result allows us to think in kinematic regions where they vanishes, independently of the values of parameters $\Delta\kappa_V$ and λ_V. In this paper we include contributions from $\tilde{\kappa}_V$, and we show that the corresponding factors $(1 \pm \cos\theta)$ and $(1 \mp \cos\theta)$ appears, respectively, indicating where to look for this special situation to measure the edm and wedm parameters.

The starting point is an effective CP-odd W-boson dipole interaction [2]

$$L = i\, g_V\, \tilde{\kappa}_V\, W_\mu^*\, W_\nu\, \tilde{V}^{\mu\nu}, \tag{1}$$

where the dual tensor $\tilde{V}_{\mu\nu}$ is defined by

$$\tilde{V}_{\mu\nu} = \frac{1}{2}\varepsilon_{\mu\nu\alpha\beta}\, V^{\alpha\beta}, \tag{2}$$

and $V_{\alpha\beta} = \partial_\alpha V_\beta - \partial_\beta V_\alpha$, W_μ^* is the field of a W^+ boson, g_V is the electric charge e ($V = \gamma$) or $g/\cos\theta_W$ ($V = Z^0$). Such form supply (weak-) electric dipole moment to the W-boson

$$d_V = \frac{g_V \tilde{\kappa}_V}{2M_W}. \tag{3}$$

The corresponding vertex is given by $ig_V \tilde{\kappa}_V \varepsilon_{\alpha\beta\mu\nu} k^\nu$, where k is the V-boson four momentum. In Fig. 1 we show the diagram where the WWV vertex enters in the process, and the contribution to the amplitude is given by

$$M_{\lambda_W \lambda_V}^{S_1 S_2} = i\, g_V\, F\, \bar{v}(\ell_2, S_2)\, \Gamma_{\mu\nu}^{\tilde{\kappa}_V} (1 - \gamma_5) \times u(\ell_1, S_1)\, \epsilon_W^{\mu *}(p, h_W)\, \epsilon_V^{\nu *}(k, h_V), \tag{4}$$

where

$$\Gamma_{\mu\nu}^{\tilde{\kappa}_V} = [(\ell_1 + \ell_2)^2 - M_W^2]^{-1}\, \tilde{\kappa}_V\, \varepsilon_{\beta\mu\nu\sigma}\, k^\sigma\, \gamma^\beta, \tag{5}$$

and $F = U_{KM} e^2 \sin^2\theta_W / 2\sqrt{2}$; v and u are the wave functions of the incoming fermions and $\epsilon_W^{\mu *}(p, h_W)$, $\epsilon_V^{\nu *}(k, h_V)$ the polarization 4-vectors of the bosons. U_{KM} is the Kobayashi-Maskawa matrix element when quarks are the elementary fermions in the reaction.

The total amplitude is given by adding to (4) the contributions from SM and anomalous $\Delta\kappa_V$ and λ_V moments, and the contributions coming from fermion exchange in the u-and t-channels [6], also shown in Fig. 1. Proceeding as usual, we compute the various angular differential cross section $d\sigma(h_W, h_V)/d\cos\theta$; from these $d\sigma(\pm, \mp)/d\cos\theta$ only receives SM contribution, $d\sigma(\pm, \pm)/d\cos\theta$ and $d\sigma(0,0)/d\cos\theta$ are dominated by the SM and $\Delta\kappa_V$ or λ_V contributions in the entire range of the angular variable. The other four contributions are the interesting ones which, after neglecting fermion masses, results in the following:

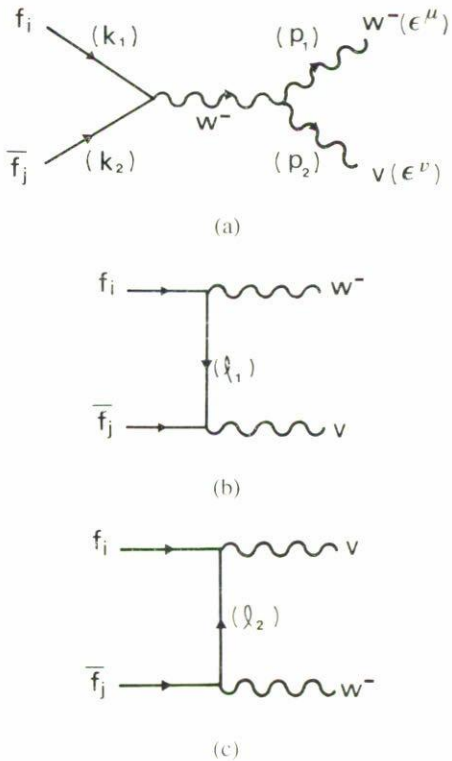

FIGURE 1. The s-channel, t-chanel and u-channel Feynman diagrams for the process $f_i \bar{f}_j \to W^\pm V$. Four-momenta are indicated in parenthesis.

$$\frac{d\sigma(\pm,0)}{d\cos\theta} = \frac{\beta}{32\pi s} F^2 \left\{ \frac{(1 - h_W \cos\theta)^2}{2r_V} \left[\left(2\lambda_W r_V - \beta + \beta_V \cos\theta + \beta \frac{\alpha - \beta\cos\theta}{1 - r_W} \right) X + 2\beta\rho Y^2 + \frac{\cot^2\theta_W}{4(1 - r_W)^2} \left(\frac{r_V}{r_W} \lambda_V \right)^2 \right] + \frac{(1 + h_W \cos\theta)^2}{32 r_V} \frac{\cot^2\theta_W}{(1 - r_W)^2} \left(\beta_V^2 - \beta^2 \right)^2 \tilde{\kappa}_V^2 \right\}; \tag{6}$$

$$\frac{d\sigma(0,\pm)}{d\cos\theta} = \frac{\beta}{32\pi s} F^2 \left\{ \frac{(1 + h_V \cos\theta)^2}{2r_W} \left\{ \left[\left(-2h_V r_W - \beta + \beta_V \cos\theta + \beta \frac{\alpha - \beta\cos\theta}{1 - r_W} \right) X + 2\beta Y \right]^2 + \frac{\cot^2\theta_W}{4(1 - r_W)^2} (\Delta\kappa_V + \lambda_V)^2 \right\} + \frac{(1 - h_V \cos\theta)^2}{32 r_W} \frac{\cot^2\theta_W}{(1 - r_W)^2} \left(\beta_V \beta_W + \beta^2 \right)^2 \tilde{\kappa}_V^2 \right\}. \tag{7}$$

In Eqs. (6) and (7) the various parameters are defined by

$$\alpha = 1 - r_W - r_V, \qquad \beta = (\alpha^2 - 4 r_W r_V)^{1/2},$$
$$\beta_W = 1 + r_W - r_V, \qquad \beta_V = 1 - r_W + r_V,$$
$$\rho = 1 + r_W + r_V,$$
$$r_W = M_W^2/s, \qquad r_V = M_V^2/s, \tag{8}$$

and

$$X = -\frac{s}{4} \left(\frac{g^i}{u} + \frac{g^j}{t} \right),$$
$$Y = -\frac{M_V^2 g^i}{4u(1 - r_W)},$$

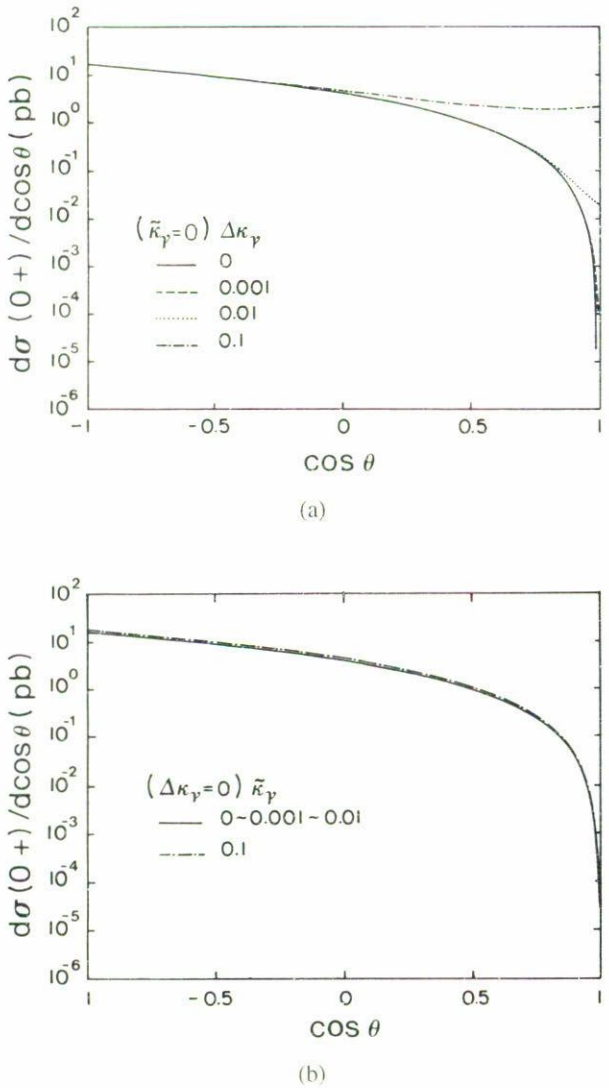

FIGURE 2. Plot of the angular differential cross-section for $e\bar{\nu}_e \to W^{\pm}\gamma$ for the helicity configuration $(0,+)$. We assume $\sqrt{s} = 200$ GeV, and (a) $\tilde{\kappa}_\gamma = 0$, $\lambda_\gamma = 0$ and several values of $\Delta\kappa_\gamma$, and (b) $\Delta\kappa_\gamma = 0$, $\lambda_\gamma = 0$ and several values of $\tilde{\kappa}_\gamma$.

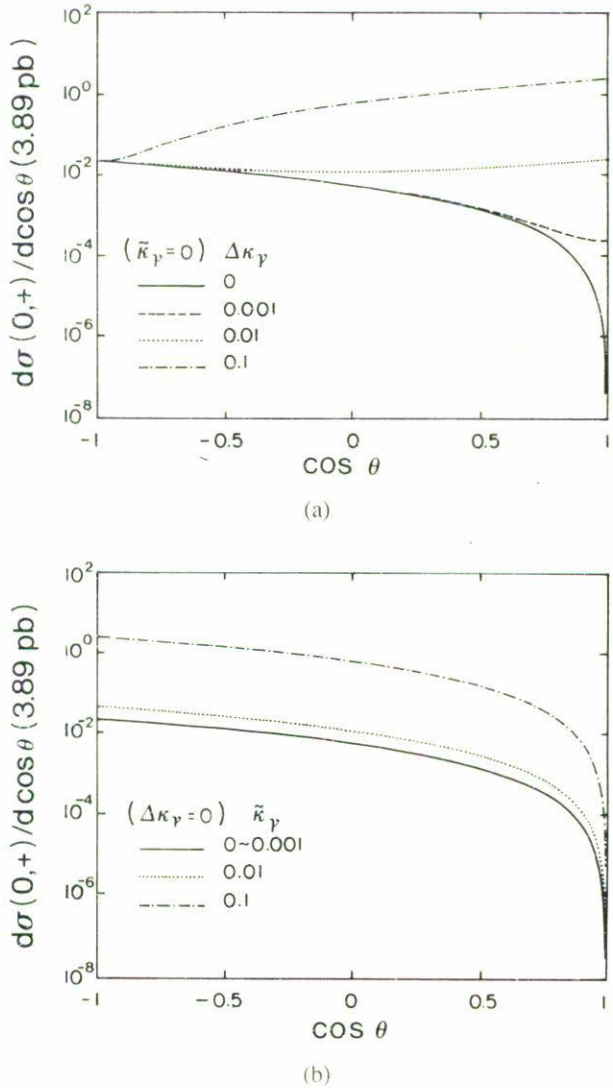

FIGURE 3. The same as in Figs. 2a–2b but with $\sqrt{s} = 1000$ GeV.

with s, t, u the Mandelstam variables, and g^i and g^j are the couplings of the fermions to the neutral boson. Next, we analize the two cases $V = \gamma, Z$.

Photon case $V = \gamma$

If in Eq. (7) we make $M_V = 0$ we obtain, for $h_\gamma = +1$,

$$\frac{d\sigma(0,+)}{d\cos\theta} = \frac{\beta}{32\pi s}F^2\left[\left(\frac{\beta^2 r_W}{2} + \frac{\cot^2\theta_W}{8r_W}\tilde{\kappa}_\gamma^2\right)(1-\cos\theta)^2 + \frac{\cot^2\theta_W}{8\beta^2 r_W}(\Delta\kappa_\gamma + \lambda_\gamma)^2(1+\cos\theta)^2\right], \quad (9)$$

showing that the effects from $\tilde{\kappa}_\gamma$ are added to those of SM contribution and can, in principle, be observed for $\cos\theta = -1$. However, this can be so only when $\tilde{\kappa}_\gamma$ takes values much bigger than 10^{-3} or we are at very high energy in order to have r_W too small to make the coefficient at the left of $\tilde{\kappa}_\gamma^2$ large enough to be competitive to the SM contribution. When $\cos\theta = +1$ the $(0,+)$ helicity gives information on $\Delta\kappa_\gamma$ and λ_γ. In Fig. 2a we have plotted Eq. (8) for the process $e\bar{\nu}_e \to W^-\gamma$, with $\sqrt{s} = 200$ GeV, $\tilde{\kappa}_\gamma = 0$, $\lambda_\gamma = 0$ and several values of $\Delta\kappa_\gamma$, showing that the effect of $\Delta\kappa_\gamma$ can be seen in $\cos\theta = +1$. In Fig. 2b the same has been done but for $\Delta\kappa_\gamma = 0$, $\lambda_\gamma = 0$, and several values of $\tilde{\kappa}_\gamma$. Here the angle of interest is $\cos\theta = -1$; however only for big values of $\tilde{\kappa}_\gamma$ we can see significant effects, as compared to the SM contribution. For greater values of $\sqrt{s}$ we have a situation where small values of the parameters can give important contributions, as can be seen in Figs. 3a–3b.

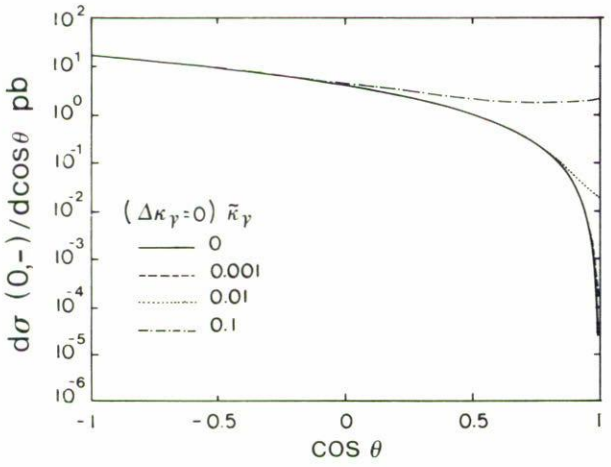

(a)

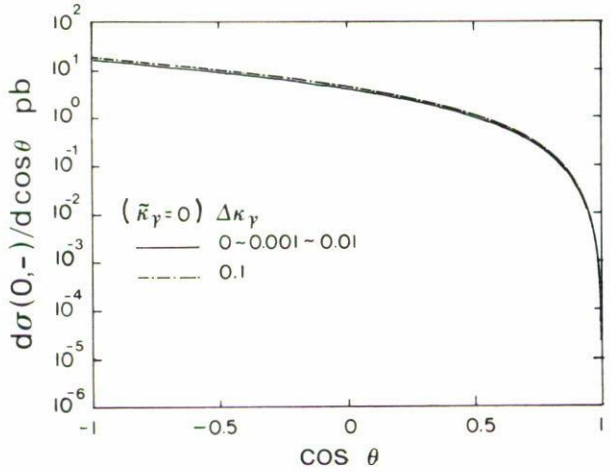

(b)

FIGURE 4. Angular differential cross-section for $e\bar{\nu}_e \to W^{\pm}\gamma$ for the helicity configuration $(0,-)$. We assume $\sqrt{s} = 200$ GeV, and (a) $\Delta\kappa_\gamma = 0$, $\lambda_\gamma = 0$ and several values of $\tilde{\kappa}_\gamma$, and (b) $\tilde{\kappa}_\gamma = 0$, $\lambda_\gamma = 0$ and several values of $\Delta\kappa_\gamma$.

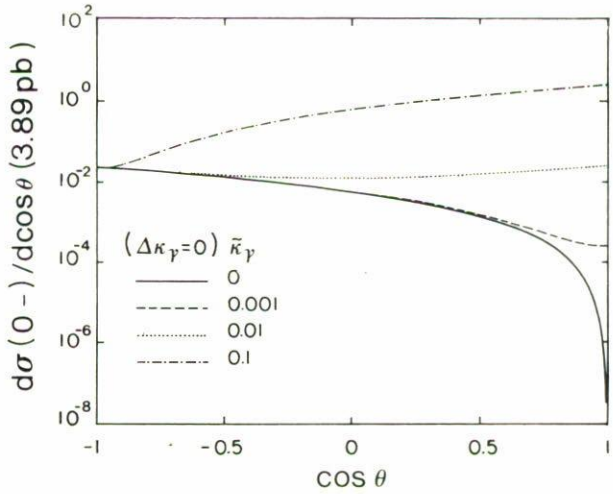

(a)

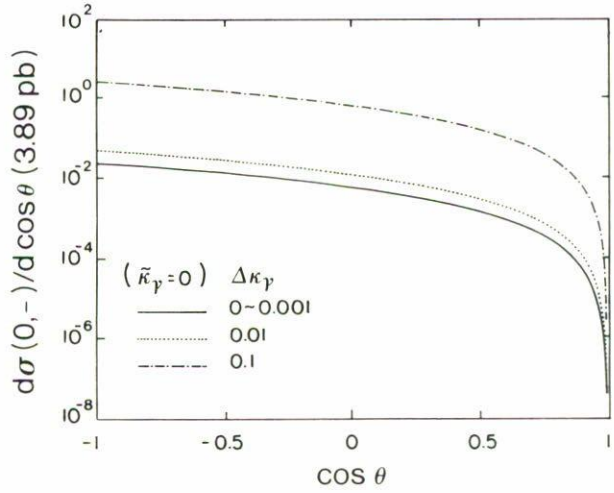

(b)

FIGURE 5. The same as in Figs. 4a–4b but with $\sqrt{s} = 1000$ GeV.

For $h_\gamma = -1$ we obtain

$$\frac{d\sigma(0,-)}{d\cos\theta} = \frac{\beta}{32\pi s}F^2\left\{\left[\frac{\beta^2 r_W}{2} + \frac{\cot^2\theta_W}{8\beta^2 r_W}(\Delta\kappa_\gamma + \lambda_\gamma)^2\right]\right.$$

$$\left.\times(1-\cos\theta)^2 + \frac{\cot^2\theta_W}{8r_W}\tilde{\kappa}_\gamma^2(1+\cos\theta)^2\right\} \quad (10)$$

Here we have the choice $\cos\theta = +1$ to get information on $\tilde{\kappa}_\gamma$ alone [7]. This is shown in Fig. 4a, for $\sqrt{s} = 200$ GeV, $\Delta\kappa_\gamma = 0$, $\lambda_\gamma = 0$ and values of $\tilde{\kappa}_\gamma$; we do the same for $\sqrt{s} = 200$ GeV, $\tilde{\kappa}_\gamma = 0$, $\lambda_\gamma = 0$ and values of $\Delta\kappa_\gamma$ in Fig. 4b. The resulting curves are quite similar to those of Figs. 2a–2b. For greater values of $\sqrt{s}$ the effects are more evident, as can be seen in Fig. 5a–5b.

Z-boson case

Analogous results for $M_V = M_Z$ are shown in Figs. 6a–6b for helicity $(0,\pm)$ and in Fig. 6c–6d for $(\pm,0)$, for the process $e\bar{\nu}_e \to W^- Z^0$ [8]. Here we have $\Delta\kappa_Z = 0$, $\lambda_Z = 0$, $\sqrt{s} = 200$ GeV, and $\tilde{\kappa}_Z = 0.001, 0.01, 0.1$. For $(0,\pm)$ we note that the effects are present at one of the extremes of the curves $\tilde{\kappa}_Z = 0.01, 0.1$, and in the modification of the quasizero, including $\tilde{\kappa}_Z = 0.001$. For $(\pm,0)$ this effects are less noticeable, and only the big value $\tilde{\kappa}_Z = 0.1$ have the effect in the dip on the curve; however, for greater values of $\sqrt{s}$ the effects are bigger, as in the previous case.

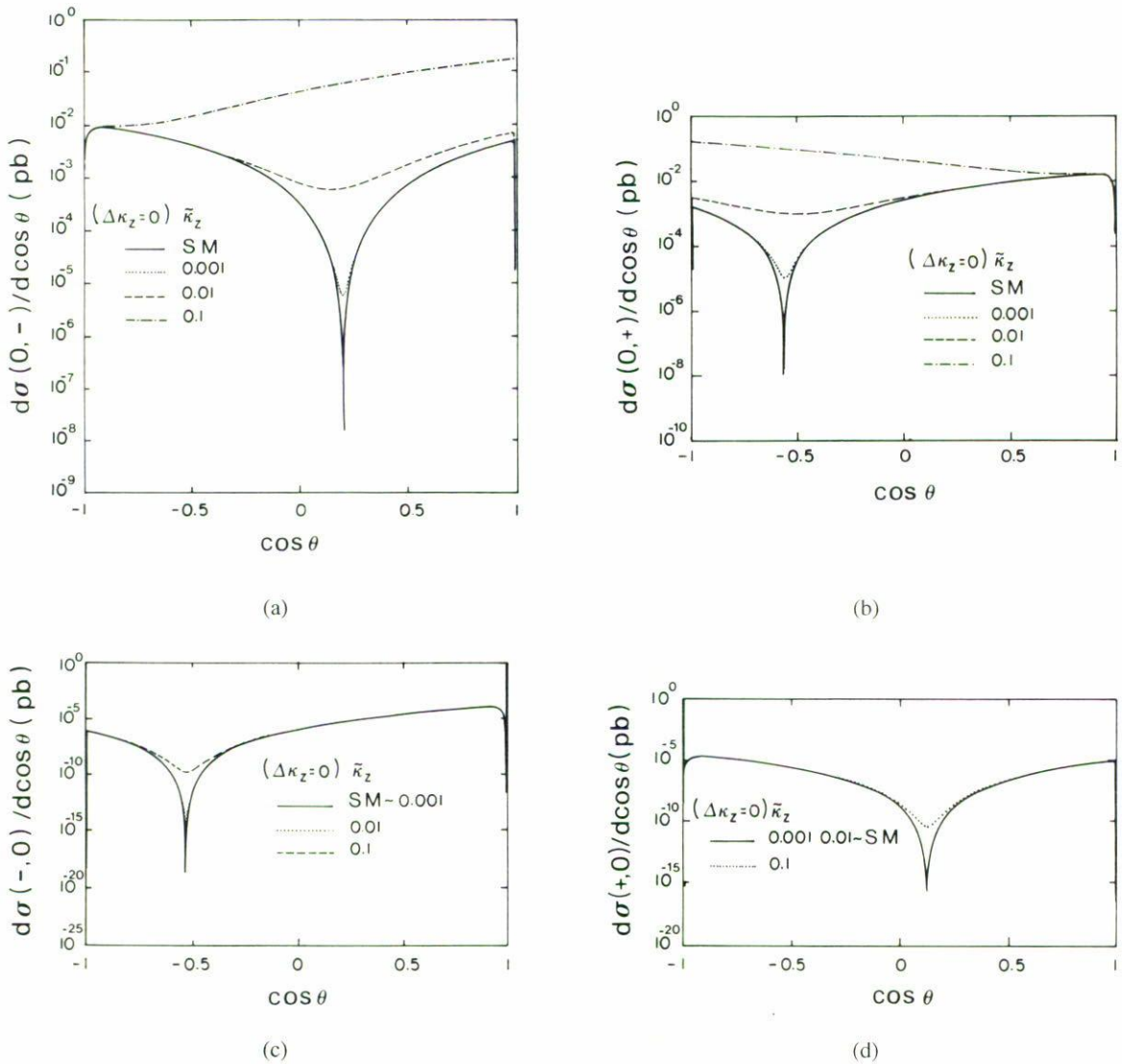

FIGURE 6. Plot of the angular differential cross-section for $e\bar{\nu}_e \to W^{\pm} Z^0$ for (a)-(b) the helicity configuration $(0, \pm)$, and (c)-(d) for $(\pm, 0)$. We assume $\sqrt{s} = 200$ GeV, $\Delta\kappa_\gamma = 0$, $\lambda_\gamma = 0$ and several values of $\tilde{\kappa}_\gamma$.

In sumary, we have complemented previous results, by others authors, to study the possibility of observing the CP-odd electric or weak-electric dipole moment of the W-boson $\tilde{\kappa}_V$ through the angular differential cross section for helicity states in the processes $f_i\bar{f}_j \to W^{\pm}\gamma$ or Z^0.

Acknowldgments

We acknowledge partial support from Comisión de Operación y Fomento de las Actividades Académicas del I.P.N., México.

1. I.B. Khriplovich and M.E. Pospelov, *Sov. J. Nucl. Phys.* **53** (1991) 638.
2. W.J. Marciano and A. Queijeiro, *Phys. Rev. D* **33** (1986) 3449.
3. A. de Rújula, M.B. Gavela, O. Pène, and F.J. Vegas, *Nucl. Phys.* **B357** (1991) 311.
4. U. Baur and D. Zeppenfeld, *Nucl. Phys.* **B308** (1988) 127.
5. F. Boudjema *et al.*, *Phys. Rev. Lett.* **36** (1989) 1906.
6. U. Baur *et al.*, *Phys. Rev. Lett.* **72** (1994) 3941, and references therein.
7. In this particular cases the zero is localized at $\cos\theta = \mp 1$ for $W^{\pm}$. For quarks in the initial state, results are quite similar, with the zero at $\cos\theta = \pm\frac{1}{3}$.
8. For this case the quasizero is at $\cos\theta = \pm\frac{1}{3}$.